Plant Physiology and Biochemistry 139 (2019) 400–410

Contents lists available at ScienceDirect

Plant Physiology and Biochemistry

journal homepage: www.elsevier.com/locate/plaphy

Research article

Phenotypic and proteomic characteristics of sorghum (*Sorghum bicolor*) albino lethal mutant *sbe6-a1*

Li Zhu[a,1], Daoping Wang[b,1], Jiusheng Sun[a,c], Yongying Mu[b], Weijun Pu[a], Bo Ma[b], Fuli Ren[a], Wenxiu Yan[b], Zhiguo Zhang[a], Guiying Li[b], Yubin Li[a,**], Yinghong Pan[b,d,*]

[a] *Biotechnology Research Institute, Chinese Academy of Agricultural Sciences, Beijing, 100081, PR China*
[b] *Institute of Crop Sciences, Chinese Academy of Agricultural Sciences, Beijing, 100081, PR China*
[c] *Research Institute of Soil, Fertilizer and Agricultural Water Conservation, Xinjiang Academy of Agricultural Sciences, Urumqi, 830091, PR China*
[d] *The National Key Facility for Crop Gene Resources and Genetic Improvement, Beijing, 100081, PR China*

ARTICLE INFO

Keywords:
Albino mutant
Chloroplast
Photosynthesis
Proteomics
Sorghum bicolor

ABSTRACT

Leaf color mutants are ideal materials for chloroplast development and photosynthetic mechanism research. Here, we characterized an EMS (ethyl methane sulfonate)-mutagenized sorghum (*Sorghum bicolor*) mutant, *sbe6-a1*, in which the severe disruption in chloroplast structure and a chlorophyll deficiency promote an albino leaf phenotype and lead to premature death. The proteomic analyses of mutant and its progenitor wild-type (WT) were performed using a Q Exactive plus Orbitrap mass spectrometer and 4,233 proteins were accurately quantitated. The function analysis showed that most of up-regulated proteins in mutant *sbe6-a1* had not been well characterized. GO-enrichment analysis of the differentially abundant proteins (DAPs) showed that up-regulated DAPs were significantly enriched in catabolic process and located in mitochondria, while down regulated DAPs were located in chloroplasts and participated in photosynthesis and some other processes. KEGG pathway-enrichment analyses indicated that the degradation and metabolic pathways of fatty acids, as well as some amino acids and secondary metabolites, were significantly enhanced in the mutant *sbe6-a1*, while photosynthesis-related pathways, some secondary metabolites' biosynthesis and ribosomal pathways were significantly inhibited. Analysis also shows that some DAPs, such as FBAs, MDHs, PEPC, ATP synthase, CABs, CHLM, PRPs, pathogenesis-related protein, sHSP, ACP2 and AOX may be closely associated with the albino phenotype. Our analysis will promote the understanding of the molecular phenomena that result in plant albino phenotypes.

1. Introduction

Chloroplast development and chlorophyll (Chl) metabolism are crucial to all photosynthetic plants. Many Chl- and chloroplast-associated mutations affecting leaf coloration and/or seedling viability have been identified in plants (Qiu et al., 2018). Leaf color variations widely exist in nature, mainly originating from spontaneous mutations (Hou et al., 2009), transposon-insertion mutants (Hayashi-Tsugane et al., 2014), T-DNA insertion mutations (Chao et al., 2014), and EMS-induced mutations (Zhu et al., 2016). The leaf color mutants can be used not only as effective markers for hybridization identification (Su et al., 2012) and molecular breeding (Qin et al., 2015), but also as ideal materials for investigating the mechanisms involved in photosynthesis, Chl biosynthesis, and chloroplast development (Li et al., 2018).

Albino mutants are the most common leaf color mutants in plants and characteristically present the inability to produce chloroplasts and defects in chloroplast developmental. The albinism phenomenon is widespread in a variety of plants, including *Arabidopsis thaliana* (de

Abbreviations: ACP2, acyl carrier protein 2; AOX, alternative oxidase; CAB, chlorophyll *a*/b binding protein; CHLM, chlorophyll magnesium-protoporphyrin IX methyltransferase; DAPs, differentially abundant proteins; EMS, ethyl methane sulfonate; FBA, Fructose-bisphosphate aldolase; GO, Gene ontology; KEGG, Kyoto Encyclopedia of Genes and Genomes; LFQ, label-free quantitative; MDH, malate dehydrogenase; MS, mass spectrometry; PEPC, phosphoenolpyruvate carboxylase; PRM, parallel reaction monitoring; PRP, plastid ribosomal protein; qRT-PCR, quantitative Real-Time Polymerase Chain Reaction; sHSP, low molecular weight heat shock protein; TEM, transmission electron microscopy; WT, wild-type

* Corresponding author. Institute of Crop Sciences, Chinese Academy of Agricultural Sciences, Beijing, 100081, PR China.
** Corresponding author.
E-mail addresses: liyubin@caas.cn (Y. Li), panyinghong@caas.cn (Y. Pan).
[1] These authors contributed equally to this work.

https://doi.org/10.1016/j.plaphy.2019.04.001
Received 11 March 2019; Accepted 1 April 2019
Available online 05 April 2019
0981-9428/

Luna-Valdez et al., 2014), rice (*Oryza sativa*) (Li et al., 2018), tobacco (*Nicotiana tabacum*) (Ye et al., 2017), barley (*Hordeum vulgare*) (Qin et al., 2015), wheat (*Triticum aestivum*) (Shi et al., 2017), and maize (*Zea mays*) (Yang et al., 2016). The underlying mechanisms related to these albino mutations are very complicated, involving in many regulatory pathways and metabolic processes (Satou et al., 2014), and also affected by the combination genetics and external environmental factors (such as cold or high temperature stress) (Gong et al., 2014; Liu et al., 2018; Lv et al., 2017; Wang et al., 2016). Plant albino mutations can be associated with the diversity of genotype (Esteves et al., 2014), or may result from mutations in genes related to chloroplast development (Wu et al., 2016; Yang et al., 2016), or the blockage of Chl biosynthetic pathway (Tominaga et al., 2016), or the defect in photosynthetic process (Zheng et al., 2016). However, the molecular mechanisms resulting in plant albinism remain elusive.

Sorghum [*Sorghum bicolor* (L.) Moench] has high photosynthetic efficiency and high biomass, and is one of the most important crops using as food, forage and biofuel in the worldwide. Because of its extensive genetic diversity, phenotypic variation, and relatively small genome size (~750 Mb), sorghum has been used as a typical C4 model crop for functional genomics research. Even though there is plant albinism, which features a deficiency of photosynthetic pigments, white seedlings are the most frequent type of Chl mutation in sorghum, and the albino factor, acting as a zygotic and gametic lethal, is inherited in a simple Mendelian recessive fashion (Karper and Conner, 1931). However, the physiological characteristics, biological bases, variations in protein abundance levels, and the molecular mechanisms regulating protein biosynthesis in albino sorghum leaves have not been fully characterized.

Proteomics presents a powerful approach for the large-scale and systematic analysis of protein expression networks and molecular regulatory mechanisms involved in plant development and environmental responses (Wang et al., 2016). The proteomics approach has been used to investigate leaf coloring mechanisms (albinism) in several higher plants (de Luna-Valdez et al., 2014; Shi et al., 2017; Wang et al., 2016). Thus, a high-throughput proteomic analysis of the albino mutants in sorghum will provide information on the underlying mechanism of leaf color variation.

In this study, we characterized a leaf color mutant, *sbe6-a1*, from a sorghum EMS-mutagenesis library that exhibits a distinct albino leaf phenotype and is eventually lethal. And then, the growth performances, Chl contents and chloroplast morphology of albino mutant and WT plant were analyzed to reveal the relationship between leaf albinism and the chloroplast-related characteristics. In addition, a proteomics approach was used to investigate the mechanism of leaf albinism. Using physiological and biochemical methods, as well as comparative proteomics, our findings increase the understanding of the molecular mechanisms involved in leaf color variants in sorghum.

2. Materials and methods

2.1. Plant materials and growth conditions

The sorghum albino mutant *sbe6-a1* was identified from an EMS-mutagenesis library of the M_3 population of sorghum cultivar Jiutian 1, which was obtained from the Biotechnology Research Institute, Chinese Academy of Agricultural Sciences. All of the sorghum seeds used in this study were propagated under standard field conditions at Langfang Experimental Base, Hebei, China. For laboratory work, sorghum plants were grown in a greenhouse under a 16 h-light/8 h-dark cycle at 28 °C in Beijing, China. No significant differences were observed between *sbe6-a1* mutant grown in the greenhouse and in the field. The growth of *sbe6-a1* mutant, owing to their inability to synthesize Chl normally, was severely inhibited, and the plants eventually died.

2.2. Chl content determination

The Chl contents were determined according to the method described by Arnon (1949). Fresh leaf discs (approximately 0.1 g fresh weight) were cut and homogenized in 80% (w/v) cold acetone, followed by centrifugation at 5,000 × *g* for 10 min. The contents of Chl *a*, Chl *b*, total Chl and carotenoids were calculated from the absorbance levels of the supernatant at 665 nm, 649 nm, and 470 nm as measured with a DU 800 UV/Vis spectrophotometer (Beckman Coulter, USA) (Lichtenthaler and Wellburn, 1987). The calculation formula is presented, and the relevant values were calculated as follows:

$$\text{Chl } a = 13.95 \times A_{665} - 6.8 \times A_{649};\ \text{Chl } b = 24.96 \times A_{649} - 7.32 \times A_{665};\ \text{Total Chl} = \text{Chl } a + \text{Chl } b = 18.16 \times A_{649} + 6.63 \times A_{665};\ \text{Carotenoid} = (1{,}000 \times A_{470} - 2.05 \times \text{Chl } a - 114.8 \times \text{Chl } b)/248$$

2.3. Transmission electron microscopy (TEM) of chloroplasts

The ultrastructure of chloroplasts from the seedling-stage leaves in the albino mutant and the WT were investigated using TEM. Fresh samples were collected from the third-leaf positions, cut into 2 mm-wide pieces, and fixed with 2.5% glutaraldehyde for 4 h at 4 °C. They were then rinsed and incubated overnight in 1% OsO_4 at 4 °C, dehydrated through a series of gradient ethanol solutions (30%, 50%, 70%, 80%, 90%, and 95%), infiltrated with a graded series of epoxy resin, and finally embedded in a pure epoxy resin at 70 °C overnight. The thick sections (90 nm) were cut into thin sections and stained with 10 mM lead citrate and 2% uranyl acetate in 50% ethanol for 10 min and then viewed using a HT7700 Transmission Electron Microscope (Hitachi, Tokyo, Japan).

2.4. Protein extraction and digestion

From each sample (two independent biological replicates and three technical repetitions), 200 mg of sorghum leaf was used for the protein extraction. Leaves were powdered in liquid nitrogen using a Cell Disruption System (Retsch, Germany) and then incubated in extraction buffer (8 M Urea, 2 M Thiourea, 2 mM EDTA, 20 mM $CaCl_2$, 500 mM NaCl, and 100 mM Tris-HCl, pH 8.1). Following sonication with an ultrasonic device (Skymen, China) at 30 KHz for 2 min at 4 °C, all of the urea-containing samples were centrifuged at 13,000 × *g* for 15 min at 4 °C, and then, the supernatants were loaded onto the filtration device (Amicon Ultra-0.5 mL Centrifugal Filters, 10 K, Millipore). The 100-mM dithiothreitol buffer was used to reduce the disulfide bonds of protein extracts after the supernatants were centrifuged at 13,000 × *g* for 25 min. After being washed with 0.3 mL of 8 M urea and 100 mM Tris-HCl (pH 8.1) buffer three times (centrifuged at 13,000 × *g* for 20 min for each wash), the protein samples were alkylated with 50 mM iodoacetamide. Following an additional three washes with 0.2 mL 8 M urea buffer (centrifuged at 13,000 × *g* for 20 min for each wash), a 50-mM NH_4CO_3 solution was added to dilute the urea agent. Then, the extracted proteins were digested with 0.5 μg trypsin (Promega, USA) for 10 h at 37 °C.

2.5. Mass spectrometry (MS) analysis

The isolation and analysis of peptide fragments were performed using the liquid chromatography system Easy nLC and the MS system Q-Excative Plus (Thermo Fisher Scientific). For each running process, 1 μL peptide sample was loaded onto a pre-separation column (P/N 164564, C18, 5-μm diameter, 100 Å pore size, 100 μm × 2 cm; Thermo Fisher Scientific) that was connected to an analytical column (P/N 164568, C18, 3-μm diameter, 100 Å pore size, 75 μm × 15 cm; Thermo Fisher Scientific). The peptide mixture was isolated by setting a gradient of

acetonitrile as follows using two solutions (solution A: 0.1% formic acid, ddH_2O; and solution B: 0.1% FA, acetonitrile): solution B, 3%–7% for 8 min, 7%–20% for 62 min; 20%–30% for 13 min; 30%–90% for 1 min, and 90% for 6 min, at a flowed rate of 400 nL min^{-1}. The parameter settings of the Data-dependent Acquisition MS were set as follows: MS spectra were acquired at resolution ratio of 70,000, scan range was set as 300 to 1,800 *m/z*, the value of AGC was acquired at $3e^6$, the injection time was set as 50 ms; the resolution ratio of MS/MS was set as 17,500 with the value of AGC set at $1e^5$, injection time was set as 45 ms, with a 27 normalized collision energy. The standard of acquisition for MS/MS was performed by collecting 20 of the most intense precursor ions and then implementing a MS/MS mass analysis. At least three replicates were performed for each experiment. The raw MS files were used for protein identification and abundance quantitation.

2.6. Protein identification and label-free quantitation

The qualitative analysis of proteins was performed using Proteome Discoverer software (version 2.1, Thermo Fisher Scientific) with Uniprot Data (*Sorghum bicolor*, 11:10 a.m., August 3, 2018). The following conditions were used: the mass tolerance of the precursor was set as 10 ppm; 0.02 Da fragment ion tolerance; up to two missed cleavages; carbamidomethyl cysteine as a fixed modification; oxidized methionine on the amino (N)-terminal; and deamination of glutamine and asparagine as variable modifications. Peptide-spectral matches were filtered to a 1% false discovery rate. Three spectral results (from three technical repetitions) were combined and searched using Proteome Discoverer software. The quantitative results were acquired using MaxQuant 1.5.3.30 software (http://www.coxdocs.org) and the phytozome database (Sbicolor_313_v3.1.protein.fa.gz, https://phytozome.jgi.doe.gov/pz/portal.html). The settings for the quantitative analysis were set as follows: the confidence of peptide fragmentation was set as high; the mass tolerance of the precursor was set as 20 ppm; 0.02 Da fragment ion tolerance; up to two missed cleavages; carbamidomethyl cysteine as a fixed modification; oxidized methionine on the amino (N)-terminal; and deamination of glutamine and asparagine as variable modifications. The qualitative and label-free quantitative (LFQ) original results obtained from the raw files were used for the subsequent bioinformatics analysis.

2.7. Bioinformatics analysis

The qualitative and label-free quantitative (LFQ) data of proteomes were pre-processed using a standardized protocol and then used for screening related proteins. The p-value threshold was set to 0.05. When the ratio of LFQ intensity of a protein in mutant *sbe6-a1* was greater than two-fold or less than half of the LFQ intensity of the same protein in the WT, then the protein was considered to be up-regulated or down-regulated, respectively. PCA (Pearson's correlation analysis) of the LFQ quantitative data was used to control the quality of the original data using the statistics software of SPSS 22.0 (https://www.ibm.com/analytics/spss-statistics-software). A Venn analysis (http://bioinfogp.cnb.csic.es/tools/venny/) was used to characterize the qualitative identification results of the mutant *sbe6-a1* and WT. Finally, the differentially abundant proteins (DAPs) between the WT and mutant were used for GO enrichment and KEGG pathway-enrichment analyses using OmicsBean (http://www.omicsbean.com).

2.8. Parallel reaction monitoring (PRM) verification

Some DAPs were verified by using PRM-MS analysis method (Peterson et al., 2012). The PRM analyses were performed on a Q-Exactive Plus mass spectrometer equipped with an Easy nLC-1000 system (Thermo Fisher Scientific, Bremen, Germany). The full MS scan was acquired with a resolution of 70,000 (at 200 *m/z*). Full MS scans were followed by 20 PRM scans at 17,500 resolution (at 200 *m/z*). The PRM analysis was employed with an isolation window of 2 Th (Thomson) for target precursor ions, and precursor ions were fragmented through higher energy collisional dissociation with normalized collision energies of 27 eV. The ACG target value was set to 3.0×10^6, and the MS scan and maximum ion injection times were set at 200 ms. The raw data obtained were then analyzed by Proteome Discoverer 2.1 (Thermo Electron, Germany) and Skyline 4.1 (https://skyline.ms).

2.9. qRT-PCR analysis

Total RNA was extracted from albino mutant and WT sorghum leaves using TRIzol reagent (TaKaRa), and cDNA was reverse transcribed from 1 μg of total RNA using a First-Strand cDNA Synthesis Kit (Invitrogen). The gene-specific primers used for qRT-PCR were designed using Primer 5 software according to cDNA sequences obtained from the Sorghum Genomics Database (v3.1.1). The sorghum actin gene was used as an endogenous control for normalization. The PCR reaction was carried out in a 20 μL volume containing 10 μL 2 × SYBR Green Master Mix reagent (TaKaRa), 1 μL cDNA template and 0.5 μL of each primer, with the following reaction conditions: 95 °C for 30 s; followed by 40 cycles of 95 °C for 10 s; 60 °C for 10 s and 72 °C for 15 s. The relative gene expression was calculated using the $2^{-\Delta\Delta Ct}$ method (Livak and Schmittgen, 2001).

A flowchart of the proteomics analysis of sorghum albino mutant and WT is illustrated in Fig. 1.

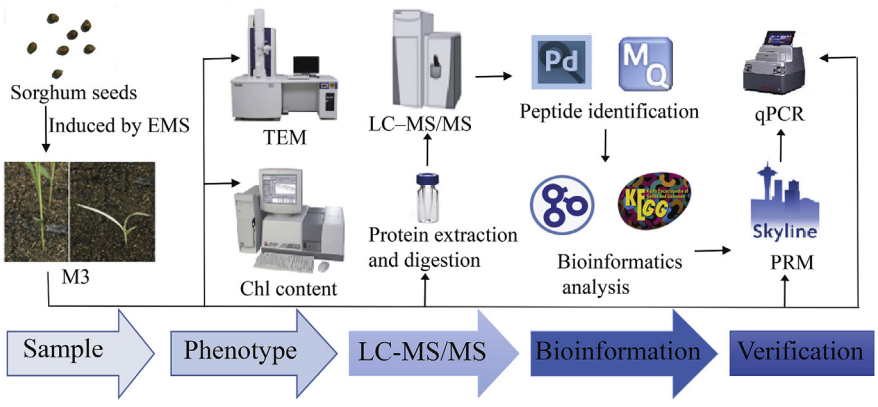

Fig. 1. The flowchart of proteomics analysis of the *sbe6-a1* mutant and WT in sorghum.

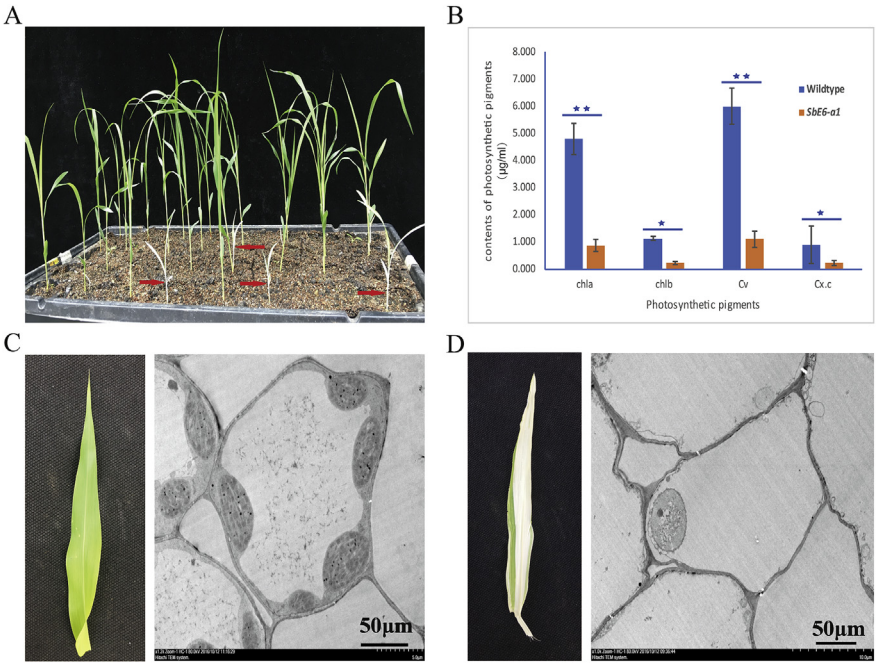

Fig. 2. Phenotypic characteristics of the albino lethal mutant *sbe6-a1* and WT at seedling-stage.

B

	M1	M2	W1	W2
M1	1	0.997	0.806	0.795
M2	0.997	1	0.809	0.798
W1	0.806	0.809	1	0.995
W2	0.795	0.798	0.995	1

C

Sample	$<10^6$	10^7	10^8	10^9	10^{10}	$>10^{10}$
M1	862	1383	1330	588	69	1
M2	907	1409	1324	535	57	1
W1	1035	1205	1295	602	93	3
W2	1287	1364	1120	405	55	2

Fig. 3. Statistical analysis of qualitatively and quantitatively identified proteins from *sbe6-a1* mutant and WT.

3. Results

3.1. Phenotypic analysis of the sorghum albino mutant

The leaf color mutant *sbe6-a1* were isolated from the segregation population of sorghum Jiutain1 EMS M_3 generation. In contrast to WT, the seedlings of *sbe6-a1* showed a distinct albinism phenomenon since seeds germination and were smaller than WT (Fig. 2A). The albino mutant grew slowly, presented albino leaf and dwarf phenotypes during plant development, and finally died. The Chl content determination data showed that the contents of Chl *a*, Chl *b*, Total Chl and carotenoids in *sbe6-a1* mutant were all drastically lower than those in the WT plants (Fig. 2B). To identify the morphological changes in the photosynthetic organelles of *sbe6-a1* leaves, the chloroplast ultrastructure was examined by TEM. The WT leaves had large and well-developed chloroplasts with grana, stromal lamellae, and thylakoid and chloroplast envelope membranes (Fig. 2C), while the chloroplasts of *sbe6-a1* exhibited abnormal morphology and distribution compared with WT (Fig. 2D).

(A) Phenotypes of the *sbe6-a1* albino mutant (red arrows) and WT in the segregation population of the EMS M_3 generation. (B) The contents of total chlorophyll, chlorophyll *a/b*, and carotenoids. Cv: Total chlorophyll content; Cx. c: carotenoids. ** indicates a significant difference at the 0.01 level; * indicates a significant difference at the 0.05 level. (C) A green leaf of a normal plant (left) and its chloroplast ultrastructure (right). (D) An albino leaf of the *sbe6-a1* mutant (left) and its chloroplast ultrastructure (right).

3.2. Qualitative and quantitative identification of proteins in leaves of the albino mutant sbe6-a1 and WT

To gain a global view of the molecular responses to albino lethal mutations, total proteins in leaves were extracted from the albino mutant *sbe6-a1* and WT plants (two independent biological replicates and three technical repetitions), and the protein expression profiles were explored by using the label-free MS-based qualitative proteomics technique. A total of 5,367 proteins were identified using the qualitative method from two biological replicates, with 4,047 proteins from the WT and 4,663 proteins from the albino mutant (Table S1). They shared 2,573 proteins in each of the biological replicates, while 1,320 proteins were identified only from the albino mutant *sbe6-a1* and 704 proteins were identified only from the WT (Fig. 3A). According to the PCA results of LFQ quantitative protein group determinations data, the correlations between the two independent biological replicates of the albino mutant *sbe6-a1* or WT were over 0.995, yet the correlations between the albino mutant *sbe6-a1* and WT in the same biological replicates were less than 0.810 (Fig. 3B). In addition, the distribution of the mass spectral intensities of the quantified proteins was mainly concentrated in the range of 10^7 to 10^8, and the numbers of the highest and the lowest abundance proteins in the mutant decreased, while the numbers of proteins in the intensity range of 10^7 to 10^8 increased when compared with WT (Fig. 3C).

(A) Venn diagram of qualitatively identified proteins from *sbe6-a1* mutant (M1 and M2) and WT (W1 and W2). Different colors in the Venn diagram indicate different plant groups. (B) Pearson's correlation analysis diagram of the quantitatively identified proteins from *sbe6-a1* mutant and WT. (C) Distribution of MS intensities of proteins identified in two independent biological replicates for the mutant *sbe6-a1* and WT.

To discover the changes of protein abundance in the analyzed mutant, all of the identified proteins were accurately quantitated, and the proteins which fold change was higher than 2 and the p-value lower than 0.05 were considered as being differentially expressed. A total of 4,233 proteins were accurately quantitated from the mutant *sbe6-a1*

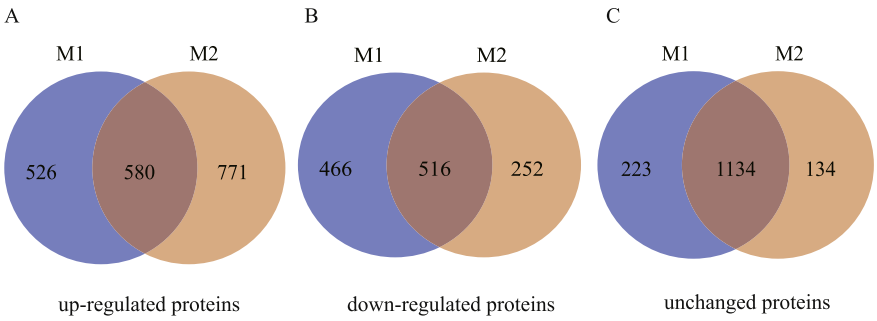

Fig. 4. Venn diagrams of DAPs identified in two independent biological replicates of the mutant *sbe6-a1* and WT. (A) Up-regulated proteins identified in *sbe6-a1 vs.* WT. (B) Down-regulated proteins identified in *sbe6-a1 vs.* WT. (C) Unchanged proteins identified in *sbe6-a1 vs.* WT. M1, M2 represent two independent biological replicates of the mutant *sbe6-a1*; W1, W2 represent two independent biological replicates of WT.

and WT (Table S2). Among them, 580 proteins were up-regulated and 516 were down-regulated, while 1,134 proteins showed no significant changes (fold change was < 2) in two independent biological replicates of the *sbe6-a1* mutant (Fig. 4).

3.3. Functional categorization of identified DAPs

The functions of all the DAPs were investigated using BLAST algorithm-based and GO enrichment analyses with OmicsBean (http://www.omicsbean.com). The GO enrichment analyses of the identified 516 down-regulated, 580 up-regulated and 1,134 unchanged proteins were performed, and the major entries of the three main GO categories, biological process, cellular component, and molecular function are shown in Fig. 5. The enrichment analysis of biological process indicated that the up-regulated proteins identified in the albino mutant were significantly enriched in catabolic processes, nucleoside metabolic processes, protein/peptide transport and localization, and other processes. In contrast, the down-regulated proteins in the albino mutant participated in photosynthesis, biosynthetic processes, metabolic processes, and the localization of chloroplasts and other organelles. The unchanged proteins took part in compound biosynthetic and metabolic processes. Putative cellular components of these MS-identified DAPs were determined through a GO analysis. The majority of up-regulated proteins were predicted to be localized in mitochondria, organelle membranes, vacuole, proteasomes, and chloroplast stroma, while the down-regulated proteins were specifically distributed in chloroplasts, plastids, photosynthetic membranes, and ribosomes. The unchanged proteins localized in many parts, including the cytoplasm, ribosomes, chloroplasts, plastids, mitochondria, and vacuoles. The analysis of the molecular functions of DAPs showed that the majority of the 580 up-regulated proteins were mapped to 181 molecular functions, including catalytic activities, hydrolase activities and molecule binding. The 516 down-regulated proteins were significantly involved in 187 molecular functions, which were related to many enzymes activities and the pigments binding, Chl binding, and other factors binding. The 1,134 unchanged proteins were significantly involved in 293 molecular functions, and they mainly participated in structural molecule activities, structural constituents of ribosomes, many enzyme activities, and the binding of nucleosides, RNA, and many other factors.

3.4. KEGG enrichment analysis of DAPs

To better understand the biological processes of the DAPs, the proteomics data were further analyzed for KEGG pathway enrichment using OmicsBean (http://www.omicsbean.com). According to the KEGG analysis of accurately quantitated proteins, 57% of the 580 up-regulated proteins, 49% of 516 down-regulated proteins, and 43% of 1,134 unchanged proteins in both of the independent biological replicates of the *sbe6-a1* mutant were annotated as “unknown function”. When comparing the total of accurately quantitated proteins, 59% of the up-regulated, 56% of the down-regulated, and 45% of the unchanged proteins were annotated as “unknown function” (Table S3 and Fig. S1). Based on the annotation information of these DAPs except the unknown function proteins, we found these 249 up-regulated proteins, 263 down-regulated proteins and 732 unchanged proteins in the albino mutant were mainly enriched in same or different pathways (Table S4). In addition, according to KEGG analysis of the DAPs, the p-values of important pathways enriched were varied between the albino mutant and WT (Table 1).

3.5. PRM and qRT-PCR verification

The results of the LFQ and bioinformatics analyses showed that many down-regulated proteins were significantly enriched in pathways related to photosynthesis. Twenty photosynthesis-related proteins and other important down-regulated proteins were selected to verify the protein expression levels determined by the PRM method using the second biological replicate sample, and the gene expression levels of 6 PRM verified proteins were further analyzed by qRT-PCR (Primers of the genes of 6 DAPs used for real-time PCR were listed in Table S6). The protein expression patterns of these 20 proteins were basically consistent with the two LFQ datasets (LFQ-1 and LFQ-2) from the two biological replicates. Unlike the protein expression patterns, only four genes (*Sobic.005G056400*, *Sobic.004G056900*, *Sobic.002G033900*, and *Sobic.003G209800*) were down-regulated, while two genes (*Sobic.005G087000* and *Sobic.009G234600*) were up-regulated in the mutant when compared with their expression levels in WT (Table 2).

4. Discussion

Albinism has been reported in many higher plant species and many albinism-responsive genes/proteins have been identified (Li et al., 2018; Shi et al., 2017). Recently, proteomics research has shifted toward the reverse genetic characterization of gene function at the proteome level. However, there are few reports related to sorghum albinism. To understand the intricate mechanisms of albinism mutations in sorghum, a proteomics analysis (LC-MS/MS) was performed to compare the EMS-induced sorghum albino mutant *sbe6-a1* with WT (Fig. 1).

Photosynthetic pigments are present in chloroplasts or photosynthetic bacteria and can capture the light energy necessary for photosynthesis. Leaf color is affected by chlorophyll and carotenoid levels in plant leaves, and leaf albinism indicates a typical Chl-deficient mutation (Li et al., 2018; Wang et al., 2016). If the biosyntheses of chlorophyll and carotenoids are suppressed and/or the synthesized chlorophyll is destroyed, then the plants are unable to produce green photosynthetic tissues. Therefore, their growth is halted, leading eventually to death. In this study, the contents of photosynthetic pigments, including Chl *a*, Chl *b*, Total Chl, and carotenoids in the leaves of mutant *sbe6-a1* were significantly lower than in WT plants (Fig. 2A and B). Thus, the albino lethal phenotype of mutant *sbe6-a1* was related to severe deficiencies in all pigments, as indicated by previous studies.

The chloroplast is a semi-autonomous organelle that contains ~100 genes and more than 3,000 proteins. A defect in chloroplast development generally results in leaf-color mutants, such as pale-green, etiolated, variegated, and albino mutants (Hayashi-Tsugane et al., 2014;

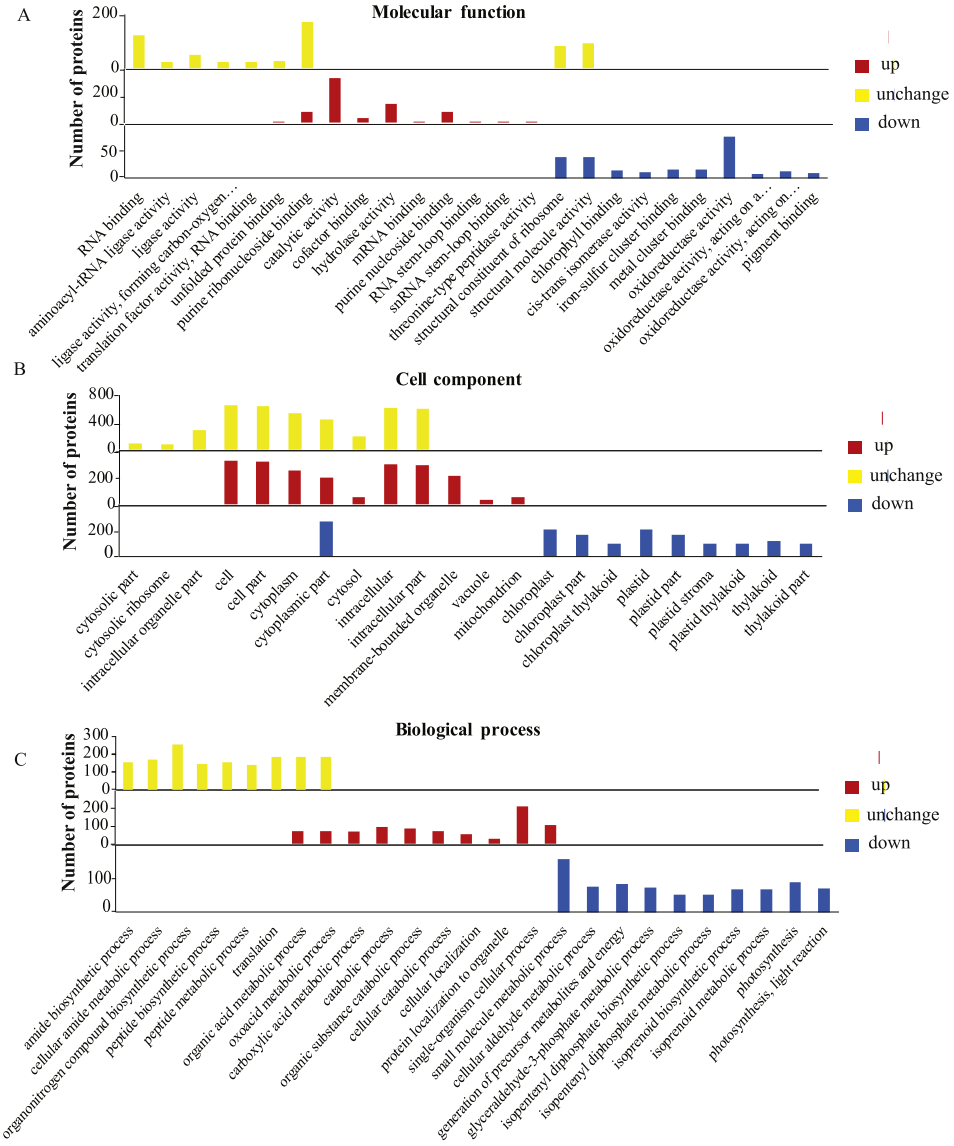

Fig. 5. GO-enrichment analysis of DAPs. The significant entries of the three GO categories, molecular function (A), cellular component (B), and biological process (C) are displayed in the horizontal coordinates. The left longitudinal coordinates represent the numbers of DAPs detected in each entry. The up-regulated proteins of *sbe6-a1 vs*. WT (red), the down-regulated proteins of *sbe6-a1 vs*. WT (blue), the unchanged proteins of *sbe6-a1 vs*. WT (yellow). (For interpretation of the references to color in this figure legend, the reader is referred to the Web version of this article.)

Pogson and Albrecht, 2011; Su et al., 2012; Sun et al., 2017). Leaf albinism is an obvious and common Chl-deficient mutation in which the most typical characteristic is that chloroplasts cannot develop normally (Wu et al., 2007). In this study, the TEM revealed that the chloroplast structures of normal plants exhibited an elliptical shape, with a typical lamellar grana and thylakoid structure (Fig. 2C). By contrast, the chloroplasts in mutant *sbe6-a1* leaves were abnormal in appearance, with a dispersed chloroplast structure (Fig. 2D). The morphological structure had obviously changed in the photosynthetic organelles of *sbe6-a1* leaves, indicating that the thylakoid membrane and grana formation in the mutant were seriously affected. So that the disintegration of chloroplast structure was one of important causes of mutant *sbe6-a1* death.

Qualitative analyses of proteomes showed that approximately 47.9% of the total identified proteins were simultaneously detected in leaves of two independent biological repeats of the albino mutant *sbe6-a1* and WT plants, and more proteins were identified from the albino mutant *sbe6-a1* (Fig. 3A). Meanwhile, quantitative analyses showed that most of proteins identified from mutant were medium abundance proteins (10^7 - 10^8) (Fig. 3C). A Pearson's correlation analysis of the four groups showed that the correlations of the quantitative proteins of the albino mutant *sbe6-a1* or the WT between two independent biological replicates was relatively high (Fig. 3B), which indicated that the experimental results are highly reproducible and can be used for subsequent bioinformatics analysis. Among the 4,233 accurately quantitated proteins, the numbers of both up-regulated and both down-regulated proteins in the two independent biological replicates of the *sbe6-a1* mutant were 580 and 516, respectively, and the total number of up-regulated proteins was significantly greater than that of down-regulated proteins (Fig. 4). These data indicated that more up-regulated proteins were detected in *sbe6-a1* mutant and they may be involved in the phenotype of the albino mutant.

GO analyses were performed on the up-regulated, down-regulated, and unchanged proteins identified in sorghum albino mutant, respectively. Most of the up-regulated proteins were localized in mitochondria, organelle membranes, vacuoles, and proteasomes, had molecular functions involving in catalytic and/or hydrolase activities, and participated in the biological processes of catabolism and nucleoside

Table 1
Important pathways enriched with up-regulated, down-regulated, and unchanged proteins of *sbe6-a1 vs*. WT.

KEGG Pathway Name	Pathway ID	P-value		
		Up-regulated	Down-regulated	Unchanged
Carbon metabolism	sbi01200	9.21E-05**	1.41E-05**	3.67E-12**
Valine, leucine and isoleucine degradation	sbi00280	1.72E-03**	0.799	0.0587
Glycolysis/Gluconeogenesis	sbi00010	1.72E-03**	0.528	6.26E-05**
Pyruvate metabolism	sbi00620	1.19E-02*	0.528	1.36E-09**
Alanine, aspartate and glutamate metabolism	sbi00250	2.28E-02*	0.777	3.92E-02*
Propanoate metabolism	sbi00640	2.28E-02*	–	1.10E-03**
Proteasome	sbi03050	2.28E-02*	–	4.51E-05**
Fatty acid degradation	sbi00071	3.54E-02*	–	0.0816
Citrate cycle (TCA cycle)	sbi00020	4.50E-02*	1	2.47E-07**
Pentose phosphate pathway	sbi00030	0.0843	2.14E-02*	0.124
Metabolic pathways	sbi01100	0.0948	1.33E-06**	5.63E-02*
Biosynthesis of amino acids	sbi01230	0.0948	3.87E-03**	1.67E-12**
Carbon fixation in photosynthetic organisms	sbi00710	0.103	8.57E-13**	2.30E-02*
Arginine biosynthesis	sbi00220	0.107	0.782	8.39E-04**
Glyoxylate and dicarboxylate metabolism	sbi00630	0.236	3.85E-03**	2.74E-04**
Oxidative phosphorylation	sbi00190	0.675	0.528	4.94E-03**
Glycine, serine and threonine metabolism	sbi00260	0.749	0.447	6.17E-03**
One carbon pool by folate	sbi00670	0.75	–	2.30E-02*
Biosynthesis of secondary metabolites	sbi01110	0.75	2.60E-04**	1.25E-02*
Ascorbate and aldarate metabolism	sbi00053	0.75	0.972	2.41E-03**
Valine, leucine and isoleucine biosynthesis	sbi00290	0.75	0.562	2.75E-06**
Glutathione metabolism	sbi00480	0.804	1	8.73E-03**
Porphyrin and chlorophyll metabolism	sbi00860	0.91	3.55E-05**	0.575
RNA transport	sbi03013	0.91	1	1.24E-02*
Pantothenate and CoA biosynthesis	sbi00770	0.946	1	2.56E-02*
Photosynthesis		1	1.85E-13**	–
Phenylalanine, tyrosine and tryptophan biosynthesis	sbi00400	1	0.877	4.33E-02*
Aminoacyl-tRNA biosynthesis	sbi00970	1	1	6.17E-03**
Ribosome	sbi03010	1	1.74E-05**	1.36E-09**
Thiamine metabolism		–	2.18E-02*	–
Photosynthesis - antenna proteins		–	6.20E-09**	–
Carotenoid biosynthesis	sbi00906	–	4.66E-02*	1
C5-Branched dibasic acid metabolism	sbi00660	–	0.777	1.37E-03**

Note: pathway enrichment analysis by p-value selection, "-" indicated the pathway was not enriched in the KEGG pathway analysis. ** indicated p-value < 0.01; * indicated p-value < 0.05. Some important KEGG enriched proteins were showed in Table S5.

metabolic processes. Most of the down-regulated proteins were localized in chloroplasts, plastids, photosynthetic membranes, and ribosomes, had molecular functions involving enzyme activities, pigment binding, and Chl binding, and mainly participated in the biological processes of photosynthesis, biosynthesis, catabolism. These results indicated that the DAPs in the mutant *sbe6-a1* were involved in different biological processes, cellular components, and molecular functions (Fig. 5). According to the KEGG-enrichment analysis of accurately quantitated proteins (Table S4), most of the DAPs related to chloroplast pigment synthesis, including photosynthesis, photosynthesis-antenna proteins, porphyrin and Chl metabolism, and carotenoid biosynthesis, were significantly decreased in albino mutant (Table 1). Thus, the distinct reduction of the Chl *a* and carotenoid contents in albino mutant (Fig. 2B) might be attributed to the down-regulation of proteins involved in Chl metabolism and carotenoid biosynthesis. A comparison of the quantitative protein accumulation revealed that the major differences between the WT and albino mutant were determined by chloroplast-related proteins at the proteomic level, in which the significant difference was that chloroplast development and photosynthesis were obviously destroyed in the albino mutant. As shown in Fig. 2, the chloroplast structure was severely damaged, and the Chl content decreased significantly in *sbe6-a1* leaves. The results indicated that these phenotypic changes in albino mutant were determined by the absence of those important photosynthesis-related proteins and energy metabolism-related proteins, and further indicated that leaf albinism was not only closely related to the damage of chloroplast structure and development, but also related to the inefficient photosynthesis.

The up- and down-regulated proteins identified in the leaves of the sorghum albino lethal mutant *sbe6-a1* were found to be associated with diverse biological processes and multiple metabolic pathway (Table 1). According to the KEGG analysis, there were approximately one-half of all quantified proteins or most of the up-regulated protein groups could not be annotated (Fig. S1), meaning that these unannotated proteins might also play important roles in the albino lethal phenotype. However, among the annotated proteins (Table S4), the up-regulated DAPs were significantly enriched in valine, leucine and isoleucine degradation and fatty acid degradation pathways, it indicated that these metabolic pathways were enhanced in the mutant. While the down-regulated DAPs were mainly enriched in the biosynthesis of amino acids, biosynthesis of secondary metabolites, carbon fixation in photosynthetic organisms, glyoxylate and dicarboxylate metabolism, metabolic pathways, and ribosome, indicating that these metabolic pathways were inhibited in the mutant. Unchanged DAPs were specifically enriched in the pathways related to aminoacyl-tRNA biosynthesis, arginine biosynthesis, ascorbate and aldarate metabolism, glutathione metabolism, glycine, serine, and threonine metabolism, one carbon pool by folate, oxidative phosphorylation, pantothenate and CoA biosynthesis, phenylalanine, tyrosine, and tryptophan biosynthesis, and RNA transport. It indicated that these basal metabolic processes may not be associated with albinism in sorghum.

Among up-regulated DAPs (Table S3), four proteins with the greatest abundance difference were obviously related to the phenotype of mutant *sbe6-a1*. They were to pathogenesis-related protein (Sobic.005G169400.1.p), low molecular weight heat shock protein (sHSP) precursor (Sobic.004G228900.1.p), acyl carrier protein 2 (ACP2) (Sobic.002G280400.1.p), and alternative oxidase (AOX) (Sobic.006G202500.1.p). Pathogenesis-related proteins usually involved in plant defense. The accumulation of pathogenesis-related proteins is

Table 2
The results of PRM and qRT-PCR verification of 20 DAPs in albino mutant *sbe6-a1*.

Protein IDs	Annotation	Pathway	LFQ 1 [M/(M + W)]	LFQ 2 [M/(M + W)]	PRM [M/(M + W)]	qRT-PCR(M/W)
Sobic.005G056400.1.p	Fructose-bisphosphate aldolase, class I	Carbon fixation in Photosynthetic organisms	0.166	0.173	0.09	0.07
Sobic.004G056900.1.p	Chlorophyll *a-b* binding protein, chloroplastic	Photosynthesis - antenna proteins	0.148	0.173	0.248	0.22
Sobic.002G033900.1.p	Photosystem I subunit X	Photosynthesis	0	0	0.224	0.62
Sobic.003G209800.1.p	Chlorophyll *a-b* binding protein, chloroplastic	Photosynthesis - antenna proteins	0.188	0.217	0.206	0.88
Sobic.005G087000.1.p	Chlorophyll *a-b* binding protein, chloroplastic	Photosynthesis - antenna proteins	0.154	0.17	0.135	1.28
Sobic.009G234600.1.p	Chlorophyll *a-b* binding protein, chloroplastic	Photosynthesis - antenna proteins	0.145	0.132	0.163	1.82
Sobic.002G338000.1.p	Light-harvesting complex II Chlorophyll *a*/b binding protein 4	Photosynthesis - antenna proteins	0.161	0.162	0.057	
Sobic.006G073500.1.p	Photosystem I subunit PsaO	Photosynthesis	0	0	0.271	
Sobic.002G004000.2.p	Photosystem II Oxygen-evolving enhancer protein 3	Photosynthesis	0.064	0.212	0.218	
Sobic.003G169100.1.p	Photosystem II CP47 reaction center protein	Photosynthesis	0.074	0.085	0.197	
Sobic.010G022100.1.p	Putative magnesium-protoporphyrin IX methyltransferase	Biosynthesis of secondary metabolites	0.086	0.063	0.282	
Sobic.010G188300.1.p	Fructose-bisphosphate aldolase, class I	Carbon fixation in photosynthetic organisms	0.089	0.112	0.278	
Sobic.002G242000.1.p	Light-harvesting complex I chlorophyll *a*/b binding protein 1	Photosynthesis - antenna proteins	0.09	0.098	0.269	
Sobic.003G159101.1.p	ATP synthase subunit beta, chloroplastic	Photosynthesis	0.109	0.109	0.022	
Sobic.004G087000.1.p	ATP synthase subunit beta, chloroplastic	Photosynthesis	0.116	0.115	0.058	
Sobic.004G235200.1.p	ATP synthase delta chain	Photosynthesis	0.136	0.116	0.276	
Sobic.008G053200.1.p	Fructose-bisphosphate aldolase	Carbon fixation in photosynthetic organisms	0.203	0.185	0.182	
Sobic.007G166300.1.p	Malate dehydrogenase	Carbon fixation in photosynthetic organisms	0.257	0.258	0.156	
Sobic.008G051000.1.p	Mg-protoporphyrin IX chelatase	Biosynthesis of secondary metabolites	0.275	0.274	0.237	
Sobic.010G160700.1.p	Phosphoenolpyruvate carboxylase 3	Carbon fixation in photosynthetic organisms	0.289	0.323	0.265	

Note: LFQ 1 and LFQ 2 represent the two quantitative datasets from two independent biological experiments.
[a] indicated that the relative gene expression was calculated using the $2^{-\Delta\Delta Ct}$ method (Livak and Schmittgen, 2001).

considered to be the principal strategies for plants in response to invading pathogens and/or stress situation (Ali et al., 2018; Chun and Chandrasekaran, 2019). sHSPs are highly conserved proteins as important member of heat shock protein (HSP) gene family, which could either protect the plant from damage caused by the stress or help repair the damage, and have vital roles in response to abiotic stresses (Wang et al., 2015; Zhang et al., 2018). ACPs have important function in synthesis of fatty acids, polyketides and non-40 ribosomal peptides, in which ACP3 was reported in involved in oxidative stress response in *pseudomonas aeruginosa(*Chen et al., 2018 *)*. AOXs are a kind of unique terminal oxidases in plant mitochondria, and can influence chloroplast energy metabolism and help plants to adapt to abiotic stress (Hu et al., 2018; Sunil et al., 2019). All these four up-regulated DAPs in mutants are found to be related to abiotic stress response. The relationship between the significantly increased expression of these defense-related proteins and the formation of albinism phenotype in sorghum mutant will be the focus of further studies.

Some down-regulated DAPs involved in carbon fixation pathway and photosynthesis should also play important roles in the formation of mutant *sbe6-a1* phenotype. Fructose-bisphosphate aldolases (FBAs) and malate dehydrogenases (MDHs) are all involved in carbon fixation pathway. FBAs are a kind of enzyme that participates in glycolysis and Calvin cycle. In this study, three FBAs (Sobic.008G053200.1.p, Sobic.005G056400.1.p, Sobic.010G188300.1.p) were identified as down-regulated proteins in the mutant, and one-of them was verified with PRM and RT-PCR. It suggested that the carbon fixation pathway maybe weakened in mutant comparing with that in WT. MDHs are a kind of critical enzymes of the C4 pathway and participate in pyruvate metabolism and carbon fixation pathway. The main role of MDHs is to catalyze the oxidative decarboxylation of malic acid to provide CO_2 for the photosynthetic carbon fixation of the Rubisco enzyme, which is closely associated with photosynthesis (Drincovich et al., 2011). Besides, NADP-MDH may related to crop abiotic stress, such as drought, low temperature, salt stress (Guo et al., 2018; Hyskova et al., 2014). In this study, one NADP-MDH (Sobic.007G166300.1.p) was identified to be down-regulated in the mutant. Moreover, phosphoenolpyruvate carboxylases (PEPCs) are a kind of cytosolic enzymes which are widely present in higher plants. In C4 and crassulacean acid metabolism (CAM) plants, PEPCs play important roles in pathways of photosynthesis, seed maturation and germination and stomatal opening (Masumoto et al., 2010; O'Leary et al., 2011). One protein (Sobic.010G160700) was identified as down-regulated PEPC in mutant *sbe6-a1* by proteomics analysis. Chloroplast ATP synthase contains nine subunits, six of which are encoded by chloroplast genes, and subunit γ, δ and II are encoded by the nuclear genes atpC, atpD and atpG, respectively. Two genes encoding γ and δ subunit of ATP synthase have been characterized in *Arabidopsis* seedling-lethal mutants (*dpa1* and *atpd*) (Dal Bosco et al., 2004; Maiwald et al., 2003), and a ATP synthase mutant *atpg* showed lethal albinism phenotype due to its inability to photoautotrophic growth (Kong et al., 2013). One δ subunit and two β subunits (encoded by Sobic.004G235200, Sobic.003G159101, Sobic.004G087000, respectively) were identified as down-regulated DAPs. It indicated that they may play important roles in albinism phenotype of mutant *sbe6-a1*. The light-harvesting chlorophyll *a*/b binding protein complex is mainly composed of chlorophyll *a*/b binding proteins (CABs) and the disruption of CABs is a mainly reason which effect on chlorophyll catabolism (Peng et al., 2013). In our stidy, six CABs (Sobic.004G056900.1.p, Sobic.003G209800.1.p, Sobic.005G087000.1.p, Sobic.009G234600.1.p, Sobic.002G242000.1.p, Sobic.002G338000.1.p) were identified as down-regulated DAPs, and some of them were verified with PRM, and the mRNA expression of two of them were verified by RT-PCR (Table 2). In chlorophyll synthesis, Mg-chelatases catalyze the insertion of Mg^{2+} into protoporphyrin IX, then Mg-protoporphyrin IX is methylated by magnesium-protoporphyrin IX methyltransferase (CHLM), which was reported to affect the stomatal aperture in *Arabidopsis thaliana* (Tomiyama et al., 2014), and finally four subsequent catalytic

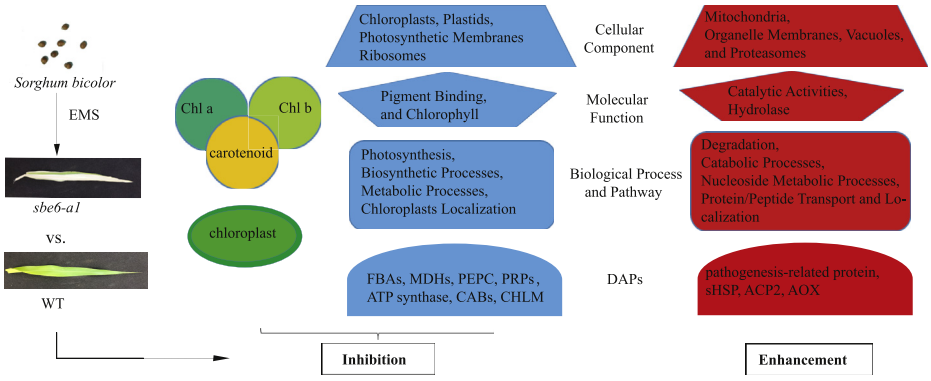

Fig. 6. Phenotypic and proteomic characteristics of the sorghum (*Sorghum bicolor*) albino lethal mutant *sbe6-a1* and wild-type. Note, the proteins such as FBAs, MDHs, PEPC, ATP synthase, CABs, CHLM and PRPs were identified to be down-regulated, and pathogenesis-related protein such as sHSP, ACP2 and AOX were up-regulated in albino mutant.

reactions produce chlorophyll *a* (Bollivar, 2006; Masuda, 2008). In mutant *sbe6-a1,* 4 proteins related to photosystem I and photosystem II were down-regulated in LFQ data and were verified with PRM. One of them was photosystem I subunit X (Sobic.002G033900) and its mRNA expression was also verified to be down-regulated. Moreover, a Mg-protoporphyrin IX chelatase (Sobic.008G051000) and a putative CHLM (Sobic.010G022100) were also verified to be down-regulated in sorghum albino mutant by using PRM. As mentioned above, the proteins involved in carbon fixation pathway such as FBAs and MDHs, and the proteins related to photosynthesis and chlorophyll synthesis such as PEPC, ATP synthase, CABs, and CHLM were all identified to be down-regulated in mutant *sbe6-a1*, and all the contents of Chl a, Chl b, Total Chl, and carotenoids in mutant were significantly lower than in WT plant. These results indicated that photosynthesis in mutant were severely weaken than in WT plant. The decrease/absence of these important proteins may affect the normal operation of pathways related to carbon fixation, photosynthesis and chlorophyll synthesis, and thus affect the normal growth and development of plants. The association between albinism and these proteins in sorghum needs to be further verified.

In addition, some other DAPs which had been proved to be related to albino phenotype in rice were also identified to be significantly down-regulated in sorghum mutant *sbe6-a1*. For example, plastid ribosomal proteins (PRPs) are important components for chloroplast biogenesis and early chloroplast development. Any defect in essential or non-essential PRPs can lead to lethality or chlorophyll deficiency in plants (Tiller and Bock, 2014; Wang et al., 2017). In this study, two proteins like PRPs (Table S3), a protein similar to PRPL11 (Sobic.001G527100.1.p) and a protein similar to PRPS6 (Sobic.001G017000.1.p) were only identified in WT, and the intensity of them were all reached to 10^8 (Table S2). It suggests that the loss of these proteins in mutants may be closely related to albinism phenotype in sorghum.

5. Conclusions

In this study, a sorghum leaf albino lethal mutant, *sbe6-a1*, was identified by screening an EMS-induced mutant pool. Compared with WT plant, the albino phenotype of the *sbe6-a1* mutant was associated with a decreased Chl content and abnormal chloroplast morphology. A proteomics analysis showed that more proteins were identified from the albino mutant *sbe6-a1*, and most of up-regulated proteins had not been well characterized. A GO-enrichment analysis of the DAPs showed that some up- and down-regulated proteins were significantly enriched in different biological processes, cellular components and molecular functions. In addition, the degradation and metabolic pathways of fatty acids, as well as some amino acids and secondary metabolites, were significantly enhanced in the mutant, while photosynthesis-related pathways and some secondary metabolites' biosynthesis, as well as ribosomal pathways, were significantly inhibited in the mutant. Analysis of existing literature shows that some DAPs, such as FBAs, MDHs, PEPC, ATP synthase, CABs, CHLM, PRPs, as well as pathogenesis/defense-related protein (including sHSP, ACP2 and AOX) may be closely associated with the albino phenotype (Fig. 6). Our analysis provides primary information that will improve the understanding of the molecular mechanisms involved in plant albino phenotypes.

Author contributions

Y.P. and L.Z. designed the research experiments; L.Z., D.W., J.S., Y.M. W.P., F.R. and W.Y. performed the experiments and analyzed the data; B.M., Z.Z. and G.L. supervised the experiments; L.Z., W.P. and B.M prepared the figures and tables; L.Z., D.W., J.S., Y.L. and Y.P. wrote the manuscript. All authors read and approved the final manuscript. The authors declare that they have no competing financial interests.

Contribution

Leaf color mutants are ideal materials for research on chloroplast development and photosynthetic mechanisms. While sorghum albino lethal mutants have been reported, their biological bases and intrinsic mechanisms are not clear. Here, we first determined that the albino phenotype of the *sbe6-a1* mutant is associated with a decreased chlorophyll content and abnormal chloroplast morphology. More differentially abundant proteins were identified from the albino mutant, and most of the up-regulated proteins had not been well characterized. Proteins with different abundance levels were enriched in different GO and KEGG pathways. We also found that some degradation and metabolic pathways were significantly enhanced in the mutants, while photosynthesis-related pathways and most biosynthetic and ribosomal pathways were significantly inhibited in the mutants. Thus, these differentially abundant proteins may be related to the albino phenotype. Our work provides new insights into the functional effects of differences in protein relative abundance levels in the leaves of the *sbe6-a1* mutant and WT.

Acknowledgments

This work was jointly supported by the “National Natural Science Foundation of China” (31471558), the “Fundamental Research Funds for Central Non-profit Scientific Institution” (Y2017PT25), the “National Key Research and Development Program of China” (2018YFD1000702), the “Agricultural Science and Technology Innovation Program” (Development and Application of Molecular Markers in Crops) and the “IAEA Coordinated Research Project” (D23031). We thank International Science Editing (http://www.internationalscienceediting.com) for editing this manuscript.

Appendix A. Supplementary data

Supplementary data to this article can be found online at https://doi.org/10.1016/j.plaphy.2019.04.001.

References

Ali, S., Ganai, B.A., Kamili, A.N., Bhat, A.A., Mir, Z.A., Bhat, J.A., Tyagi, A., Islam, S.T., Mushtaq, M., Yadav, P., Rawat, S., Grover, A., 2018. Pathogenesis-related proteins and peptides as promising tools for engineering plants with multiple stress tolerance. Microbiol. Res. 212, 29–37. https://doi.org/10.1016/j.micres.2018.04.008.

Arnon, D.I., 1949. Copper enzymes in isolated chloroplasts. Polyphenoloxidase in Beta Vulgaris. Plant Physiol 24, 1–15. https://doi.org/10.1104/pp.24.1.1.

Bollivar, D.W., 2006. Recent advances in chlorophyll biosynthesis. Photosynth. Res. 90, 173–194. https://doi.org/10.1007/pl00022068.

Chao, Y., Kang, J., Zhang, T., Yang, Q., Gruber, M.Y., Sun, Y., 2014. Disruption of the homogentisate solanesyltransferase gene results in albino and dwarf phenotypes and root, trichome and stomata defects in Arabidopsis thaliana. PLoS One 9, e94031. https://doi.org/10.1371/journal.pone.0094031.

Chen, W., Wang, B., Gruber, J.D., Zhang, Y.M., Davies, C., 2018. Acyl carrier protein 3 is involved in oxidative stress response in Pseudomonas aeruginosa. Front. Microbiol. 9, 2244. https://doi.org/10.3389/fmicb.2018.02244.

Chun, S.C., Chandrasekaran, M., 2019. Chitosan and chitosan nanoparticles induced expression of pathogenesis-related proteins genes enhances biotic stress tolerance in tomato. Int. J. Biol. Macromol. 125, 948–954. https://doi.org/10.1016/j.ijbiomac.2018.12.167.

Dal Bosco, C., Lezhneva, L., Biehl, A., Leister, D., Strotmann, H., Wanner, G., Meurer, J., 2004. Inactivation of the chloroplast ATP synthase gamma subunit results in high non-photochemical fluorescence quenching and altered nuclear gene expression in Arabidopsis thaliana. J. Biol. Chem. 279, 1060–1069. https://doi.org/10.1074/jbc.M308435200.

de Luna-Valdez, L.A., Martinez-Batallar, A.G., Hernandez-Ortiz, M., Encarnacion-Gueuara, S., Ramos-Vega, M., Lopez-Bucio, J.S., Leon, P., Guevara-Garcia, A.A., 2014. Proteomic analysis of chloroplast biogenesis (clb) mutants uncovers novel proteins potentially involved in the development of Arabidopsis thaliana chloroplasts. J. Proteom. 111, 148–164. https://doi.org/10.1016/j.jprot.2014.07.003.

Drincovich, M.F., Lara, M.V., Andreo, C.S., Maurino, V.G., 2011. Chapter 14 C4 decarboxylases: different solutions for the same biochemical problem, the provision of CO2 to Rubisco in the bundle sheath cells. In: Raghavendra, A.S., Sage, R.F. (Eds.), C4 Photosynthesis and Related CO2 Concentrating Mechanisms. Springer, Netherlands, Dordrecht, pp. 277–300. https://doi.org/10.1007/978-90-481-9407-0_14.

Esteves, P., Clermont, I., Marchand, S., Belzile, F., 2014. Improving the efficiency of isolated microspore culture in six-row spring barley: II-exploring novel growth regulators to maximize embryogenesis and reduce albinism. Plant Cell Rep. 33, 871–879. https://doi.org/10.1007/s00299-014-1563-1.

Gong, X.D., Su, Q.Q., Lin, D.Z., Jiang, Q., Xu, J.L., Zhang, J.H., Teng, S., Dong, Y.J., 2014. The rice OsV4 encoding a novel pentatricopeptide repeat protein is required for chloroplast development during the early leaf stage under cold stress. J. Integr. Plant Biol. 56, 400–410. https://doi.org/10.1111/jipb.12138.

Guo, Y.Y., Song, Y.S., Zheng, H.X., Zhang, Y., Guo, J.R., Sui, N., 2018. NADP-malate dehydrogenase of sweet sorghum improves salt tolerance of Arabidopsis thaliana. J. Agric. Food Chem. 66, 5992–6002. https://doi.org/10.1021/acs.jafc.8b02159.

Hayashi-Tsugane, M., Takahara, H., Ahmed, N., Himi, E., Takagi, K., Iida, S., Tsugane, K., Maekawa, M., 2014. A mutable Albino allele in rice reveals that formation of thylakoid membranes requires the SNOW-white LEAF1 gene. Plant Cell Physiol. 55, 3–15. https://doi.org/10.1093/pcp/pct149.

Hou, D.Y., Xu, H., Du, G.Y., Lin, J.T., Duan, M., Guo, A.G., 2009. Proteome analysis of chloroplast proteins in stage albinism line of winter wheat (triticum aestivum) FA85. Bmb Rep. 42, 450–455. https://doi.org/10.5483/Bmbrep.2009.42.7.450.

Hu, W.H., Yan, X.H., He, Y., Ye, X.L., 2018. Role of alternative oxidase pathway in protection against drought-induced photoinhibition in pepper leaves. Photosynthetica 56, 1297–1303. https://doi.org/10.1007/s11099-018-0837-1.

Hyskova, V.D., Miedzinska, L., Dobra, J., Vankova, R., Ryslava, H., 2014. Phosphoenolpyruvate carboxylase, NADP-malic enzyme, and pyruvate, phosphate dikinase are involved in the acclimation of Nicotiana tabacum L. to drought stress. J. Plant Physiol. 171, 19–25. https://doi.org/10.1016/j.jplph.2013.10.017.

Karper, R.E., Conner, A.B., 1931. Inheritance of chlorophyll characters in sorghum. Genetics 16, 291–308. https://doi.org/10.1007/BF02983936.

Kong, M.M., Wang, F.F., Yang, Z.N., Mi, H.L., 2013. ATPG is required for the accumulation and function of chloroplast ATP synthase in Arabidopsis. Chin. Sci. Bull. 58, 3224–3232. https://doi.org/10.1007/s11434-013-5916-x.

Li, H.C., Ji, G.B., Wang, Y., Qian, Q., Xu, J.C., Sodmergen, Liu, G.Z., Zhao, X.F., Chen, M.S., Zhai, W.X., Li, D.Y., Zhu, L.H., 2018. WHITE PANICLE3, a novel nucleus-encoded mitochondrial protein, is essential for proper development and maintenance of chloroplasts and mitochondria in rice. Front. Plant Sci. 9 doi:Artn 762 10.3389/Fpls.2018.00762.

Lichtenthaler, H.K., Wellburn, A.R., 1987. Chlorophyll and carotenoids, pigments of photosynthetic biomembranes. Methods Enzymol 148, 350–382. https://doi.org/10.1016/0076-6879(87)48036-1.

Liu, X., Lan, J., Huang, Y.S., Cao, P.H., Zhou, C.L., Ren, Y.K., He, N.Q., Liu, S.J., Tian, Y.L., Nguyen, T., Jiang, L., Wan, J.M., 2018. WSL5, a pentatricopeptide repeat protein, is essential for chloroplast biogenesis in rice under cold stress. J. Exp. Bot. 69https://doi.org/10.1093/jxb/ery214. 4495-4495.

Livak, K.J., Schmittgen, T.D., 2001. Analysis of relative gene expression data using real-time quantitative PCR and the 2(T)(-Delta Delta C) method. Methods 25, 402–408. https://doi.org/10.1006/meth.2001.

Lv, Y., Shao, G., Qiu, J., Jiao, G., Sheng, Z., Xie, L., Wu, Y., Tang, S., Wei, X., Hu, P., 2017. White Leaf and Panicle 2, encoding a PEP-associated protein, is required for chloroplast biogenesis under heat stress in rice. J. Exp. Bot. 68, 5147–5160. https://doi.org/10.1093/jxb/erx332.

Maiwald, D., Dietzmann, A., Jahns, P., Pesaresi, P., Joliot, P., Joliot, A., Levin, J.Z., Salamini, F., Leister, D., 2003. Knock-out of the genes coding for the Rieske protein and the ATP-synthase delta-subunit of Arabidopsis. Effects on photosynthesis, thylakoid protein composition, and nuclear chloroplast gene expression. Plant Physiol. 133, 191–202. https://doi.org/10.1104/pp.103.024190.

Masuda, T., 2008. Recent overview of the Mg branch of the tetrapyrrole biosynthesis leading to chlorophylls. Photosynth. Res. 96, 121–143. https://doi.org/10.1007/s11120-008-9291-4.

Masumoto, C., Miyazawa, S., Ohkawa, H., Fukuda, T., Taniguchi, Y., Murayama, S., Kusano, M., Saito, K., Fukayama, H., Miyao, M., 2010. Phosphoenolpyruvate carboxylase intrinsically located in the chloroplast of rice plays a crucial role in ammonium assimilation. Proc. Natl. Acad. Sci. U. S. A. 107, 5226–5231. https://doi.org/10.1073/pnas.0913127107.

O'Leary, B., Park, J., Plaxton, W.C., 2011. The remarkable diversity of plant PEPC (phosphoenolpyruvate carboxylase): recent insights into the physiological functions and post-translational controls of non-photosynthetic PEPCs. Biochem. J. 436, 15–34. https://doi.org/10.1042/BJ20110078.

Peng, G., Xie, X.L., Jiang, Q., Song, S., Xu, C.J., 2013. Chlorophyll a/b binding protein plays a key role in natural and ethylene-induced degreening of Ponkan (Citrus reticulata Blanco). Sci Hortic-Amsterdam 160, 37–43. https://doi.org/10.1016/j.scienta.2913.05.022.

Peterson, A.C., Russell, J.D., Bailey, D.J., Westphall, M.S., Coon, J.J., 2012. Parallel reaction monitoring for high resolution and high mass accuracy quantitative, targeted proteomics. Mol. Cell. Proteomic 11 (11), 1475–1488. https://doi.org/10.1074/mcp.O112.020131.

Pogson, B.J., Albrecht, V., 2011. Genetic dissection of chloroplast biogenesis and development: an overview. Plant Physiol. 155, 1545–1551. https://doi.org/10.1104/pp.110.170365.

Qin, D., Dong, J., Xu, F., Guo, G., Ge, S., Xu, Q., Xu, Y., Li, M., 2015. Characterization and fine mapping of a novel barley stage green-revertible albino gene (HvSGRA) by bulked segregant analysis based on SSR assay and specific length Amplified fragment sequencing. BMC Genomics 16, 838. https://doi.org/10.1186/s12864-015-2015-1.

Qiu, Z., Chen, D., Lei, H., Zhang, S., Yang, Z., Yu, Z., Wang, Z., Ren, D., Qian, Q., Guo, L., 2018. The rice white green leaf 2 gene causes defects in chloroplast development and affects the plastid ribosomal protein S9. Rice 11, 39. https://doi.org/10.1186/s12284-018-0233-2.

Satou, M., Enoki, H., Oikawa, A., Ohta, D., Saito, K., Hachiya, T., Sakakibara, H., Kusano, M., Fukushima, A., Saito, K., 2014. Integrated analysis of transcriptome and metabolome of Arabidopsisalbino or pale green mutants with disrupted nuclear-encoded chloroplast proteins. Plant Mol. Biol. 85, 411–428. https://doi.org/10.1007/s11103-014-0194-9.

Shi, K., Gu, J., Guo, H., 2017. Transcriptome and proteomic analyses reveal multiple differences associated with chloroplast development in the spaceflight-induced wheat albino mutantmta. PLoS One 12. https://doi.org/10.1371/journal.pone.0177992.

Su, N., Hu, M.L., Wu, D.X., Wu, F.Q., Fei, G.L., Lan, Y., Chen, X.L., Shu, X.L., Zhang, X., Guo, X.P., Cheng, Z.J., Lei, C.L., Qi, C.K., Jiang, L., Wang, H., Wan, J.M., 2012. Disruption of a rice pentatricopeptide repeat protein causes a seedling-specific albino phenotype and its utilization to enhance seed purity in hybrid rice production. Plant Physiol. 159, 227–238. https://doi.org/10.1104/pp.112.195081.

Sun, L., Wang, Y., Liu, L., Wang, C., Gan, T., Zhang, Z., Wang, Y., Wang, D., Niu, M., Long, W., 2017. Isolation and characterization of a spotted leaf 32 mutant with early leaf senescence and enhanced defense response in rice. Sci. Rep. 7, 41846. https://doi.org/10.1038/srep41846.

Sunil, B., Saini, D., Bapatla, R.B., Aswani, V., Raghavendra, A.S., 2019. Photorespiration is complemented by cyclic electron flow and the alternative oxidase pathway to optimize photosynthesis and protect against abiotic stress. Photosynth. Res. 139, 67–79. https://doi.org/10.1007/s11120-018-0577-x.

Tiller, N., Bock, R., 2014. The translational apparatus of plastids and its role in plant development. Mol. Plant 7, 1105–1120. https://doi.org/10.1093/mp/ssu022.

Tominaga, J., Mizutani, H., Horikawa, D., Nakahara, Y., Takami, T., Sakamoto, W., Sakamoto, A., Shimada, H., 2016. Rice CYO1, an ortholog of Arabidopsis thaliana cotyledon chloroplast biogenesis factor AtCYO1, is expressed in leaves and involved in photosynthetic performance. J. Plant Physiol. 207, 78–83. https://doi.org/10.1016/j.jplph.2016.10.005.

Tomiyama, M., Inoue, S., Tsuzuki, T., Soda, M., Morimoto, S., Okigaki, Y., Ohishi, T., Mochizuki, N., Takahashi, K., Kinoshita, T., 2014. Mg-chelatase I subunit 1 and Mg-protoporphyrin IX methyltransferase affect the stomatal aperture in Arabidopsis thaliana. J. Plant Res. 127, 553–563. https://doi.org/10.1007/s10265-014-0636-0.

Wang, A., Yu, X., Mao, Y., Liu, Y., Liu, G., Liu, Y., Niu, X., Altpeter, F., 2015. Overexpression of a small heat-shock-protein gene enhances tolerance to abiotic stresses in rice. Plant Breed. 134, 384–393. https://doi.org/10.1111/pbr.12289.

Wang, W.J., Zheng, K.L., Gong, X.D., Xu, J.L., Huang, J.R., Lin, D.Z., Dong, Y.J., 2017. The rice TCD11 encoding plastid ribosomal protein S6 is essential for chloroplast development at low temperature. Plant Sci. 259, 1–11. https://doi.org/10.1016/j.plantsci.2017.02.007.

Wang, Y., Zhang, J., Shi, X., Peng, Y., Li, P., Lin, D., Dong, Y., Teng, S., 2016. Temperature-sensitive albino gene TCD5, encoding a monooxygenase, affects chloroplast development at low temperatures. J. Exp. Bot. 67, 5187–5202. https://doi.org/10.1093/jxb/erw287.

Wu, L., Wu, J., Liu, Y., Gong, X., Xu, J., Lin, D., Dong, Y., 2016. The rice pentatricopeptide

repeat gene TCD10 is needed for chloroplast development under cold stress. Rice 9, 67. https://doi.org/10.1186/s12284-016-0134-1.

Wu, Z.M., Zhang, X., He, B., Diao, L.P., Sheng, S.L., Wang, J.L., Guo, X.P., Su, N., Wang, L.F., Jiang, L., Wang, C.M., Zhai, H.Q., Wan, J.M., 2007. A chlorophyll-deficient rice mutant with impaired chlorophyllide esterification in chlorophyll biosynthesis. Plant Physiol. 145, 29–40. https://doi.org/10.1104/pp.107.100321.

Yang, J., Suzuki, M., Mccarty, D.R., 2016. Essential role of conserved DUF177A protein in plastid 23S rRNA accumulation and plant embryogenesis. J. Exp. Bot. 67, 5447–5460. https://doi.org/10.1093/jxb/erw311.

Ye, L.S., Zhang, Q., Pan, H., Huang, C., Yang, Z.N., Yu, Q.B., 2017. EMB2738, which encodes a putative plastid-targeted GTP-binding protein, is essential for embryogenesis and chloroplast development in higher plants. Physiol. Plantarum 161. https://doi.org/10.1111/ppl.12603.

Zhang, L., Hu, W., Gao, Y., Pan, H., Zhang, Q., 2018. A cytosolic class II small heat shock protein, PfHSP17.2, confers resistance to heat, cold, and salt stresses in transgenic Arabidopsis. Genet. Mol. Biol. 41, 649–660. https://doi.org/10.1590/1678-4685-GMB-2017-0206.

Zheng, K., Jian, Z., Lin, D., Chen, J., Xu, J., Hua, Z., Sheng, T., Dong, Y., 2016. The rice TCM5 gene encoding a novel deg protease protein is essential for chloroplast development under high temperatures. Rice 9, 1–13. https://doi.org/10.1186/s12284-016-0086-5.

Zhu, X., Shuang, G., Wang, Z., Du, Q., Xing, Y., Zhang, T., Shen, W., Sang, X., Ling, Y., He, G., 2016. Map-based cloning and functional analysis of YGL8 , which controls leaf colour in rice (Oryza sativa). BMC Plant Biol. 16, 134. https://doi.org/10.1186/s12870-016-0821-5.